9118 *Macromolecules* **2009**, *42*, 9118–9123
DOI: 10.1021/ma901316k

Macromolecules
ARTICLE

UCST Responsive Microgels of Poly(acrylamide−acrylic acid) Copolymers: Structure and Viscoelastic Properties

Coro Echeverria, Daniel López, and Carmen Mijangos*

Instituto de Ciencia y Tecnología de Polímeros, CSIC, Juan de la Cierva 3, 28006 Madrid, Spain

Received June 18, 2009; Revised Manuscript Received September 25, 2009

ABSTRACT: Positive thermosensitive microgels were obtained via the inverse emulsion polymerization method with controlled feeding system. Random acrylamide and acrylic acid copolymer microgels with different compositions were synthesized and characterized. Dynamic light scattering was used to determine the hydrodynamic diameter and swelling behavior. The morphology, distribution, and size were determined by scanning electron microscopy (SEM). Cross-linker and acrylic acid concentration of the copolymer affected collapse temperature of the swelling behavior. An oscillatory rheometer was used to study the viscoelastic properties. The viscoelastic modulus G', and G'', of the microgel nanoparticle dispersions suggested a solidlike behavior. A scaling theory was applied to describe the structure of microgel dispersion, and the fractal dimension of the aggregates was obtained.

Introduction

Microgels are intramolecularly cross-linked polymer particles in colloidal size range. Being sensitive to environmental conditions (temperature, pH, electric field, magnetic field, ionic strength), microgels swell and deswell in suitable solvents in response to external stimuli.[1,2]

In recent years these smart microgels have received growing attention due to their potential applications in numerous fields, such as drug delivery, sensors, catalysis, chemical separation, and enzyme immobilization.[3−9]Numerous reports have been focused on temperature-sensitive[10,11] microgels with negative thermosensitivity.[12] Thus, the particle deswells with increasing temperature, usually closely related to the lower critical solution temperature (LCST) of the corresponding polymer. *N*-Isopropylacrylamide is the most well-studied system in which the volume phase transition (VPT) is driven by hydrophobic interactions between the macromolecules.[13]

However, there are certain applications for which a positive thermosensitivity is needed. In this case, this behavior is related to the upper critical solution temperature (UCST) of the polymer.[14] One of the systems with positive thermosensitivity is microgels composed of acrylamide and acrylic acid. Recently, it has been reported by Peppas et al. and previously by Bouillot and Vincent that their volume change with temperature is driven by hydrogen bonding that causes the microgel to shrink at temperatures below the UCST and swell at temperatures above the UCST.[15,16]

It has also been reported that, compared to macrogels, microgels have a surface-to-volume much high interfacial area per unit mass of gel,[17] which means greater exchange rates. Therefore, morphology and monodispersity[18] are very important in order to improve their performance in the aforementioned applications.

At the moment, there are few reports concerning the study of the rheological properties of negative thermosensitive microgels. In the case of microgels based on poly(*N*-isopropylacrylamide), studies were mainly focused on the flow behavior[19,20] and the effective volume fraction of the particles.[21,22] However, it is indeed important to understand the contribution of microgel particles into the colloidal dispersion, how they affect the rheological behavior of the system, and which the influence of the concentration into the viscoelastic properties is. From this study, information about the interactions and elasticity in the structure of the microgel dispersion could be inferred. In regard to that, other papers have been published related to the rheological properties of non-polymeric systems, from where the interaction and fractal dimension can be deduced.[23,24]

Taking into account these studies, and the previous studies of our group on rheological properties of gels,[25−30] in this paper we tried to correlate the structure of a microgel dispersion to their viscoelastic properties. For that, in this work we prepared positively thermosensitive monodisperse random copolymer microgels of poly(acrylamide−acrylic acid) and characterized the morphology, thermally responsive swelling properties, and the viscoelastic properties. The effect of acrylic acid−acrylamide ratio as well as the effect of cross-linker concentration in the swelling behavior was studied. Finally, the contribution of the intrinsic elasticity of microgel particles to the viscoelastic properties of the dispersion was also studied. A fractal analysis of the system was carried out to find out the more suitable model to explain the structure of the microgel dispersion.

Experimental Section

Materials. Acrylamide (AA, Aldrich) and acrylic acid (AAc, Aldrich) were used as monomer and comonomer, respectively. *N*,*N*′-Methylenebis(acrylamide) (MBA, Aldrich) was used as the cross-linking agent. 2,2′-Azobis(2-methylpropionamidine) dihydrochloride (AMPA-d, Aldrich) was the initiator of the reaction. Span 80 (Sorbitan monooleate) (Fluka) and dodecane (Fluka) were employed as surfactant and organic solvent, respectively. Water used in the preparation and characterization of microgels was Millipore Milli-Q grade.

Polymerization Reaction. Microgel particles were synthesized by inverse emulsion polymerization (w/o) method, in which the aqueous phase was dispersed into the oil phase forming water droplets. The polymerization was thermally initiated using 2,2′-azobis(2-methylpropionamidine dihydrochloride) (AMPA-d) as initiator.

*Corresponding author. E-mail: cmijangos@ictp.csic.es.

 Published on Web 10/27/2009

Table 1. Recipes Used for the Production of the Microgels[a]

	aqueous phase					organic phase		initiator
	monomer (M)	comonomer (CM)		cross-linker (X)		($m_{dodecane}/m_{SPAN80}$ = 2.25%)		I
reactions	AA (mol)	AAc (mol)	AAc (wt % M)	MBA (mol)	MBA (wt % M)	dodecane (mL)	SPAN80 (g)	AMPA-d (wt % M)
PAA−AAc−0% AAc−5% MBA	0.056			1.29×10^{-3}	5	30	0.5056	1
PAA−AAc−0.5% AAc−5% MBA	0.056	2.77×10^{-4}	0.5	1.29×10^{-3}	5	30	0.5056	1
PAA−AAc−1% AAC−5% MBA	0.056	5.55×10^{-4}	1	1.29×10^{-3}	5	30	0.5056	1
PAA−AAc−2% AAc−5% MBA	0.056	1.11×10^{-3}	2	1.29×10^{-3}	5	30	0.5056	1
PAA−AAc−2% AAc−2% MBA	0.056	1.11×10^{-3}	2	5.19×10^{-4}	2	30	0.5056	1
PAA−AAc−2% AAc−10% MBA	0.056	1.11×10^{-3}	2	2.59×10^{-3}	10	30	0.5056	1
PAA−AAc−4% AAc−5% MBA	0.056	2.22×10^{-3}	4	1.29×10^{-3}	5	30	0.5056	1

[a] Reaction conditions: 475 rpm; reaction time = 3 h; reaction temperature = 50 °C.

For the oil phase, emulsifier (SPAN 80) and the organic solvent (dodecane) were mixed. The acrylamide (AA) monomer, the cross-linker *N*,*N*′-methylenebis(acrylamide) (MBA), and acrylic acid (AAc) comonomer were dissolved in the aqueous phase. Both solutions were purged with nitrogen for half an hour before starting the polymerization reaction. Once the organic phase was charged into a three-neck round-bottom flask, the aqueous phase was added to the flask in a controlled manner at 1.5 mL/min by means of a peristaltic pump in order to help the droplets formation to be of a similar size. The flask content was heated at the desired temperature and stirred at 475 rpm agitation rate. After adding the initiator, the mixture became immediately turbid, and the polymerization reaction was allowed to continue under a nitrogen atmosphere, with stirring for 3 h. The reaction was then cooled to room temperature while stirring and nitrogen flow were maintained to avoid aggregation.

Finally, the prepared materials were purified by removal of the organic phase and precipitation of the aqueous phase in ethanol with subsequent washing by centrifugation.

All samples were redispersed in deionized water and placed in dialysis bags (molecular weight cutoff = 3500) for 1 week to remove any unreacted materials.

Different microgel particles were prepared by varying the amount of cross-linker and comonomer. Table 1 shows the recipes and reaction conditions in the production of the cross-linked poly(acrylamide−acrylic acid) microgels. Samples were defined as PAA−AAc−*X* AAc−*Y* MBA, with *X* referring to the acrylic acid wt % and *Y* referring to the cross-linker wt %.

Characterization of the PAA−AAc Microgels. The hydrodynamic diameter of the microgels was determined as a function of temperature via temperature-programmed dynamic light scattering (Malvern Nanosizer Nano S). The measurements were performed in 1 °C increments from 15 to 45 °C with 10 min of thermal stabilization at each temperature with the samples at pH 5.

To visualize the morphology and particle size in the dried state of the microgel particles, environmental scanning electron microscopy (XL30 ESEM, Philips) was used. Purified samples redispersed in deionized water were prepared for imaging. A drop of 10^{-4} wt % of microgels dispersion was deposited in a glass wafer, dried, and sputter-coated with gold to minimize charging at fixed conditions.

Rheological studies of 1, 2, and 5 wt % microgel dispersions of the representative sample PAA−AAc−2% MBA−2% AAc were carried out using the AR-G2 TA Instruments stress-controlled oscillatory rheometer. The dispersions were prepared dissolving the dried microgels in the distilled water. All the samples were prepared separately (2 mL of sample) in order to avoid any error in the concentration. The geometry used was 60 mm parallel plate. Frequency sweep test were carried out in the linear viscoelastic regime at 20 °C. Also, strain sweep tests at a constant, nondestructive, frequency were carried out.

Results and Discussion

Synthesis of different poly(acrylamide−acrylic acid) microgels were obtained by inverse emulsion polymerization under controlling feeding rate varying acrylic acid and cross-linker concentration (see Table 1). This allowed us to control the composition, the size, and the distribution of microgels. For a concentration of 4% of acrylic acid a nonhomogeneous system was obtained.

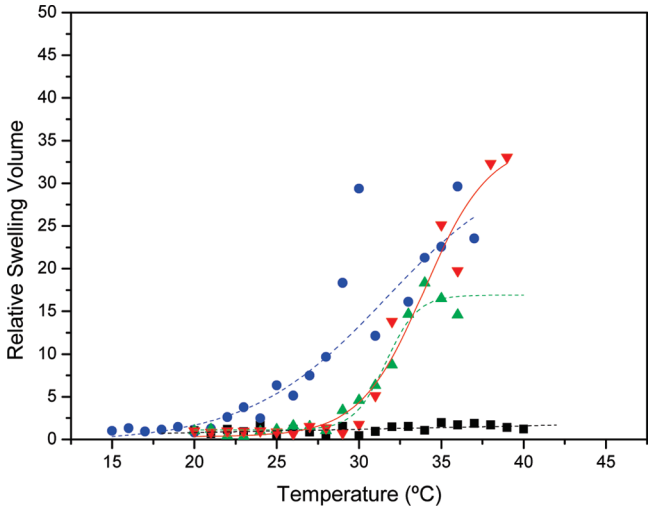

Figure 1. Dynamic light scattering plot of thermally responsive microgels as a function of the acrylic acid concentration: (■) 0% AAc−5% MBA; (●) 0.5% AAc−5% MBA; (▲) 1% AAc−5% MBA; (▼) 2% AAc−5% MBA.

Swelling Behavior of Microgels. Dynamic light scattering was used to examine the effect of polymeric structure on the swelling properties of various cross-linked poly(acrylamide−acrylic acid) microgels. As shown in both Figure 1 and Figure 2, microgels shrink at temperatures below the UCST and swell at temperatures above the UCST, revealing a positively thermosensitive volume phase transition. This transition can be attributed to hydrogen-bonding driven forces between PAA and AAc.[15,16] At temperatures below the UCST hydrogen-bonding forces dominate and maintain the particles in a collapsed state; however, as the temperature increases, these bonds weaken and a hydrophilic front is set up within the microgel, giving rise to the swelling of microgel. In the study of these UCST type microgels it is important to know the influence of the acrylic acid in the hydrodynamic diameter of the microgel particles. In Figure 1 the relative swelling volume (RSV), that is, the average volume of swollen particles at a specific temperature over the average volume of the particles in the collapsed state, is plotted as a function of temperature. From this graph it is observed that (i) polyacrylamide microgels do not show UCST behavior, (ii) a 0.5 wt % of acrylic acid provokes the copolymer to be thermosensitive, and (iii) the increase of acrylic acid in the composition of the microgel leads to a shift to higher values

in the collapse temperature. It is worth mentioning the important increase of 10 °C with the acrylic acid concentration variation from 0.5 to 2%. The UCST or collapse temperature is determined as the intercept point between the two slopes, and the values obtained for the different systems are summarized in Table 2.

These results can be interpreted by considering that the volume phase transition of this system is driven by hydrogen bonding, as stated before and explained in the following way. As the acrylic acid in the system increases, the number of hydrogen bonds is higher; therefore, the mobility of the chains should decrease, leading to a delay in temperature of the collapse. These results will be confirmed by SEM.

Another parameter studied in the UCST behavior of acrylamide−acrylic acid microgels is the influence of the cross-linker concentration. In Figure 2 the relative swelling volume with temperature for samples containing different concentration of cross-linker is represented. The cross-linking degree affects both the relative swelling and the volume phase transition temperature. Besides, the sample containing 10% of cross-linker undergoes a slightly lower swelling at temperatures above the UCST with respect to the other two samples with a 2 and 5 wt % cross-linking. Concerning the volume phase transition temperature, the increase of cross-linking degree provokes a shift toward lower temperatures of the collapse. These results can be explained by the fact that an increment of the cross-linker decreases the mesh size and therefore could affect the mobility of the chains able to form hydrogen bonds, hindering the formation of these bonds and hence shifting volume phase transition to lower temperature. These results will also be confirmed by SEM. Collapse temperatures of the samples are also summarized in Table 2.

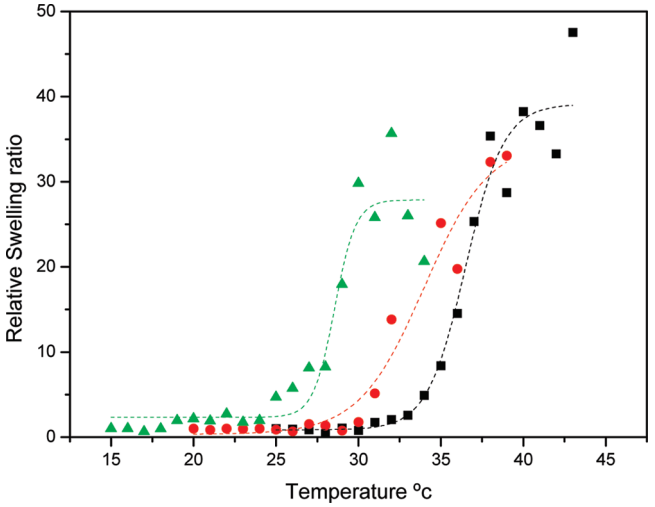

Figure 2. Dynamic light scattering plot of thermally responsive microgels as a function of cross-linker concentration: (■) 2% AAc−2% MBA; (●) 2% AAc−5% MBA; (▲) 2% AAc−10% MBA.

Table 2. Collapse Temperature of Poly(AA−AAc) Microgels as a Function of Acrylic Acid Concentration and MBA Cross-Linker Concentration

influence of AAC (%)		influence of cross-linker (%)	
acrylic acid (%)	collapse temperature (°C)	MBA (%)	collapse temperature (°C)
0		2	32
0.5	21	5	30
1	28	10	24
2	31		

Morphology and Size of Microgels. In the study of the microgels morphology, SEM images give the necessary information regarding homogeneity, monodispersity, and size.

Figure 3 shows representative SEM images of diluted (10^{-4} g/mL) microgel dispersions corresponding to the samples PAA−AAc−2% AAc−5% MBA (A and B) and PAA−AAc−2% AAc−2% MBA (C). Both samples present a spherical shape and are highly monodisperse in size. This monodispersity can also be observed at large scale in Figure 3B. The size obtained for PAA−AAc−2% AAc−5% MBA is 374 nm, whereas the size obtained for the PAA−AAc−2% AAc−2% MBA is 296 nm.

The influence of both the cross-linker and the acrylic acid concentration in the microgel morphology was also elucidated through SEM. In Figure 4 SEM micrographs corresponding to five different samples are shown. Comparing micrographs A, B, and C, it is observed that as the cross-linker concentration increases from micrograph A to C, the diameter of the dried particles decreases. With respect to micrographs D and E, a slight decrease in the particle size is observed as the concentration of acrylic acid increases. Sizes obtained from micrographs are summarized in Table 3. Although the obtained values are not exactly the same (samples are in dried state), this observation confirms the results obtained from DLS.

Viscoelastic Properties. As it is known, a gel should be characterized by an elastic modulus at zero frequency. Therefore, the viscoelastic characterization could be performed from frequency sweeps. In order to determine the viscoelastic properties of the microgel dispersions, PAA−AAc−2% MBA−2% AAc was chosen as representative sample, and the concentrations of microgel dispersions were 1, 2, and 5 wt %.

Strictly speaking, the frequency-dependent storage modulus G' and loss modulus G'' were measured under oscillatory shear, in the linear viscoelastic regime at 20 °C. The measurements for this colloidal dispersion were done in a relatively short frequency range in order to avoid the inertia of the

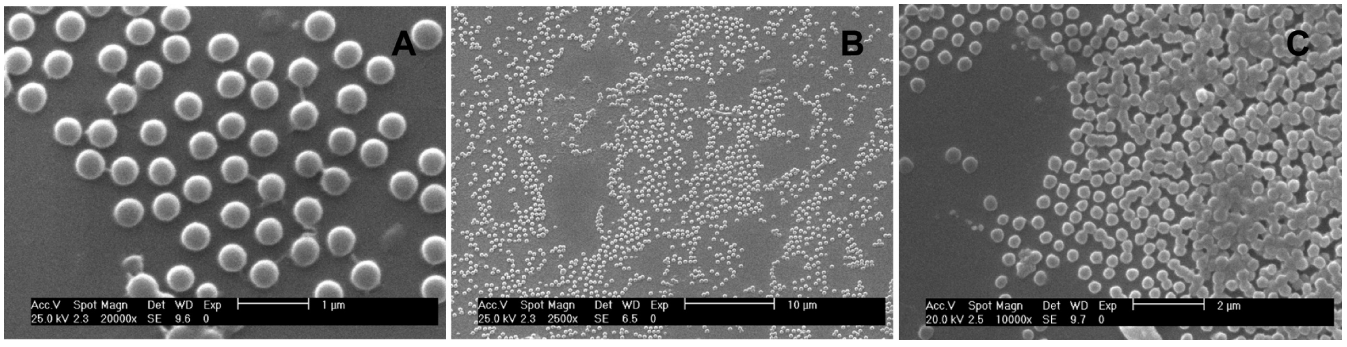

Figure 3. SEM Micrographs of PAA−AAc−2% AAc−5% MBA: (A) scale of 1 μm; (B) scale of 10 μm; (C) PAA−AAc−2% AAc−2% MBA.

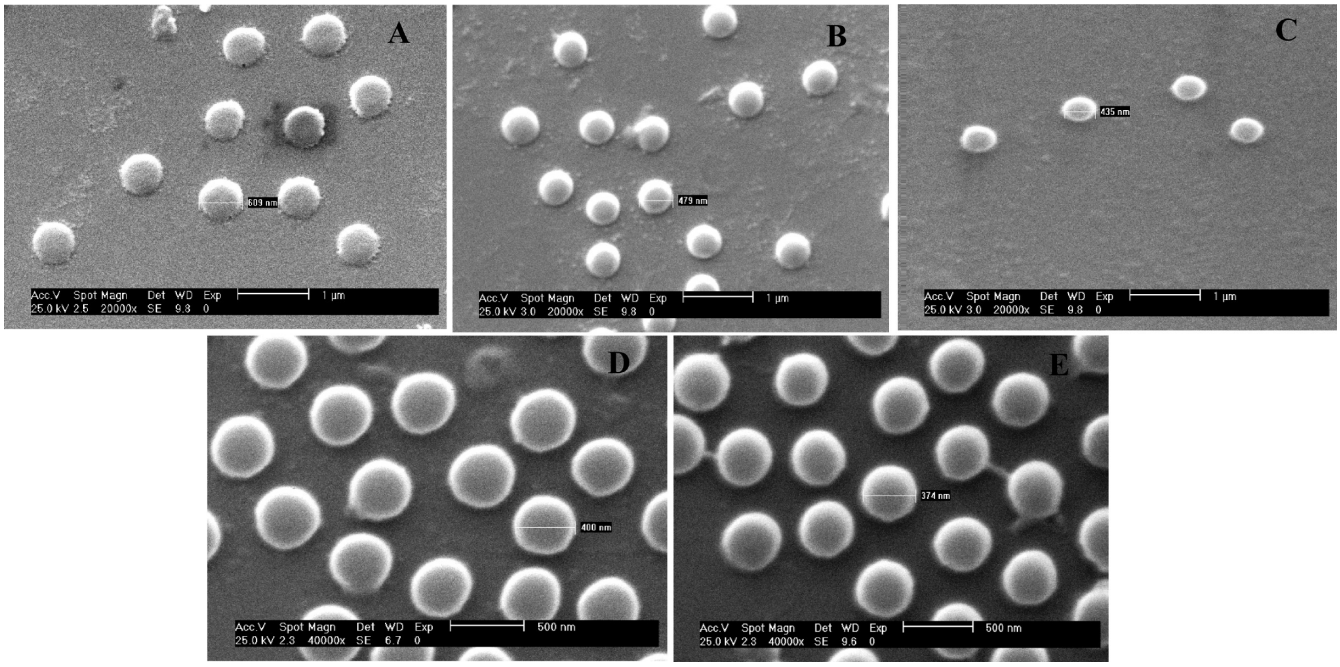

Figure 4. SEM micrographs of samples containing (A) PAA−AAc−0.5% AAc−2% MBA, (B) PAA−AAc−0.5% AAc−5% MBA, (C) PAA−AAc−0.5% AAc−10% MBA, (D) PAA−AAc−1% AAc−5% MBA, and (E) PAA−AAc−2% AAc−5% MBA.

Table 3. Diameter of Dried Samples Measured from SEM Micrographs

sample	D (nm)
PAA−AAc−0.5% AAc−2% MBA	609
PAA−AAc−0.5% AAc−5% MBA	479
PAA−AAc−0.5% AAc−10% BA	435
PAA−AAc−1% AAc−5% MBA	400
PAA−AAc−2% AAc−5% MBA	374

rheometer, since this inertia could provoke results that would not correspond to the sample behavior.

In Figure 5 is represented the frequency sweep test of dispersions of the sample PAA−AAc−2% MBA−2% AAc of concentrations 1 and 5 wt %. It is observed that the elastic modulus is independent of the frequency and that the elastic component (G') of both dispersions is higher than the viscous one (G'') which is characteristic of gel behavior. Additionally, if we compare the two samples of concentrations 1 and 5 wt %, it is observed that dispersion containing higher microgel content shows a higher elastic modulus. Below the 1 wt % of microgel particles the colloidal suspension is dispersed, and therefore no flocs are formed.

In order to deepen in the viscoelastic characterization of the system, up and down strain sweep tests at a constant, nondestructive, frequency were carried out for the representative sample PAA−AAc−2% MBA−2% AAc, as is shown in Figure 6. The concentrations of the microgel dispersion chosen were 1, 2, and 5 wt %. It can be easily observed that the more concentrated the dispersion is, the higher is the value obtained for the elastic modulus.

For the sample of 5 wt %, it is observed that increasing the applied strain, the elastic modulus keeps constant up to a value where the linearity is broken, and almost the crossover point ($G' = G''$) is achieved. If we go back in the measurement, from this nonlinear value, decreasing the applied strain, it is observed that the sample is able to recover and even to superimpose the elastic modulus plateau obtained in the first sweep. However, for less concentrated samples, there is a slight difference of the elastic modulus plateau on the up and

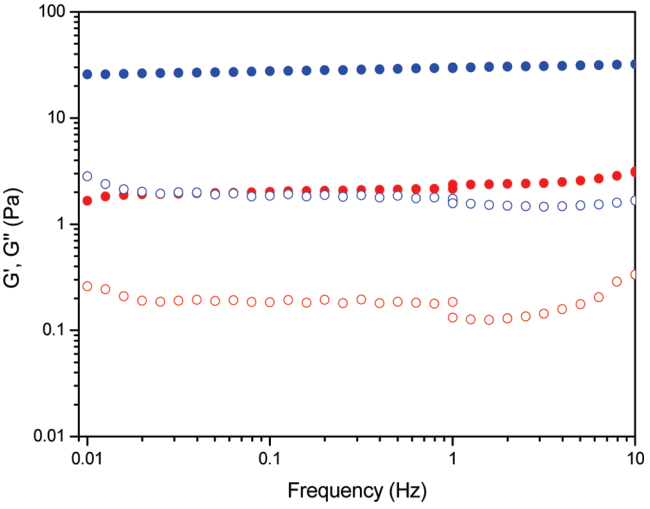

Figure 5. Storage modulus (full symbols) and loss modulus (open symbols) as a function of frequency of PAA−AAc−2% MBA−2% AAc microgel dispersions of 1 wt % (red) and 5 wt % (blue) concentration. At 1 Hz, the applied strain is changed in order to maintain the linear viscoelastic regime.

down sweep. From this graph we can also extract that the linear viscoelastic region increases with the concentration.

Considering the results obtained from both frequency and strain sweep tests, we can describe the system as a microgel dispersion that forms a kind of structure giving rise to solidlike viscoelastic behavior (see Scheme 1A). The question is whether the elasticity of the colloidal gel is mainly due to the intrinsic elasticity of the microgel particles or, on the contrary, to interactions among particles.

The structure of the colloidal gel is highly disordered, but at a certain length scales they are often self-similar and can be described in terms of fractal geometry.[31] Thus, fractal analysis is a suitable tool to study the colloidal structure and to elucidate this dilemma. To determine the structure of a colloidal gel from rheological measurements, it is necessary

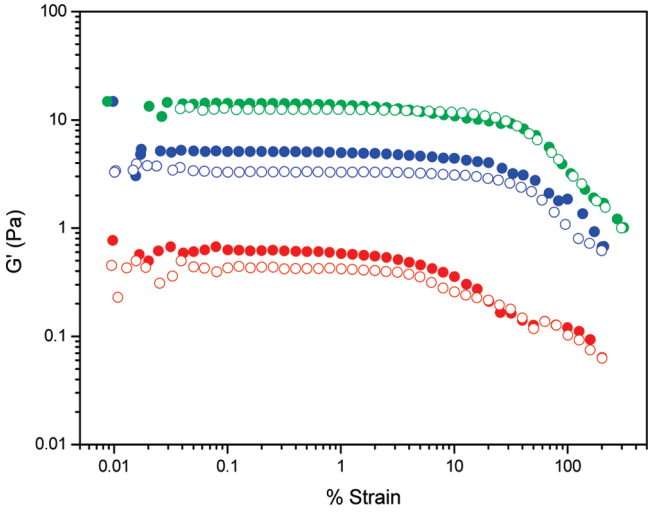

Figure 6. Elastic modulus (G') as a function of strain in a up (full symbol) and down (open symbol) sweep test of PAA−AAc−2% MBA−2% AAc microgel dispersions of 1 (red), 2 (blue), and 5 wt % (green) concentration.

Scheme 1. (A) Microgel Dispersion Sample Represented Schematically; (B) Representation of the Scaling Model[a]

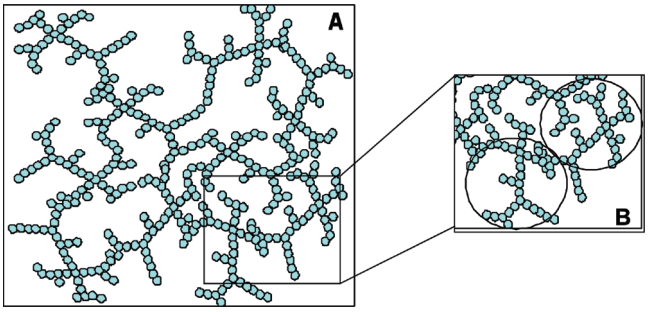

[a] The circles indicate fractal flocs, and the regions between flocs are considered as links.

to apply the scaling theory that relates it to their elastic properties.

The scaling theory considers the structure of the colloidal gel as a collection of flocs (fractal objects closely packed throughout the sample) (see Scheme 1B). The first theory in which aggregated structures are related with their rheological properties was developed by Brown and Ball.[23] Shih et al. extended this model and developed a scaling model by defining two separate regimes: strong-link regime and weak-link regime.[24]

In the strong-link regime, the links between flocs (inter) are stronger than the intrinsic elasticity of aggregates (intra). The elastic modulus plateau (G'_0) and the limit of linearity (γ_0) or critical deformation (the deformation at which the elastic modulus starts to decrease) are related with the concentration as follows:

$$G'_0 \approx \varphi^{(d+x)/(d-D)} \tag{1}$$

$$\gamma_0 \approx \varphi^{-(1+x)/(d-D)} \tag{2}$$

where φ is the concentration, d is the Euclidean dimension of the system ($d = 3$), D is the fractal dimension, and x is some number that is less than the fractal dimension and larger than the unity.

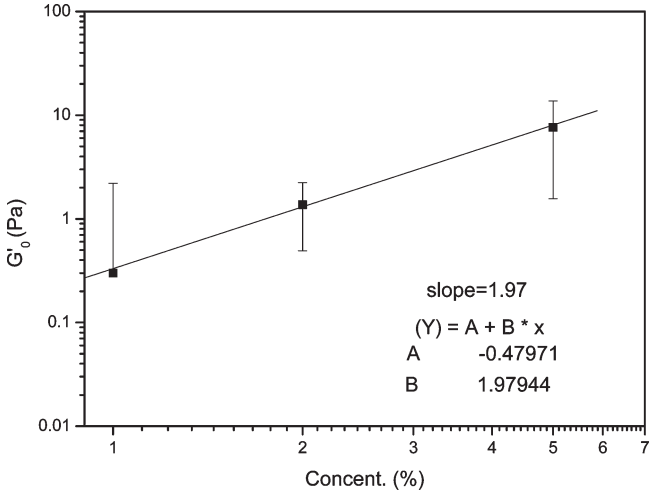

Figure 7. Elastic modulus plateau (G') as a function of concentration for sample PAA−AAc−2% MBA−2% AAc.

For the weak-link regime, the elastic modulus is dominated by the elasticity of the aggregates, rather than the interlinks between aggregates. In this case, the elastic modulus and the limit of linearity are related to the concentration as

$$G'_0 \approx \varphi^{(d-2)/(d-D)} \tag{3}$$

$$\gamma_0 \approx \varphi^{1/(d-D)} \tag{4}$$

The comparison of both regimes, comparing the exponents of eq 1 with eq 3 and eq 2 with eq 4, allows to deduce that in the weak-link regime the elastic modulus increases slowly compared to the strong-link and also that the limit of linearity increases with concentration.

We have represented in Figures 7 and 8 the storage modulus plateau G'_0 and the critical deformation γ_0 as a function of the microgel concentration, respectively. Both G'_0 and γ_0 show a power-law behavior and can be approximated to the forms

$$G'_0 \approx \varphi^{1.97} \tag{5}$$

$$\gamma_0 \approx \varphi^{1.40} \tag{6}$$

It is worth mentioning that the results show high error bars. However, the main conclusion comes from the qualitative analysis of the trend of the slope. The trend allows us to determine whether the system is under a strong-like or weak-like regime. The error could affect to the accuracy of the fractal dimension but not the behavior of the system.

From Figure 8 it is observed that the limit of linearity increases with the concentration of the dispersion. This trend clearly indicates that the system is in the weak-link regime. Subsequently, as the model predicts, the elasticity of the system is mainly due to the elastic constant of the flocs (intra) and not to interflocs interactions. These results suggest that microgel particles interact and aggregate forming these flocs or structure that give rise to a gel behavior. Although we cannot precise the kind of interactions among the aggregates, these are weak and therefore flocs can break and recover easily. From these equations it is possible to obtain an

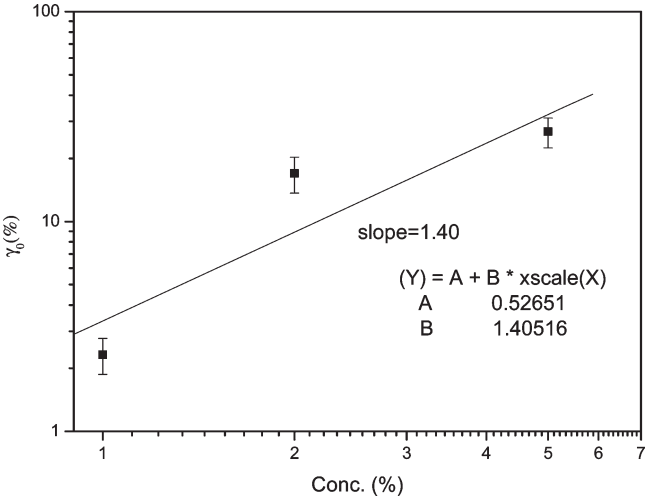

Figure 8. Critical deformation (γ_0) as a function of concentration for sample PAA−AAc−2% MBA−2% AAc.

approximate value for the fractal dimension of the flocs (aggregates); thus, comparing eq 4 with eq 6, one obtains that $D \sim 2.28$. This value suggests that the degree of particle densification in the aggregates (flocs) is high.

Conclusions

Thermosensitive monodisperse random copolymer microgels of poly(acrylamide−acrylic acid) were synthesized by an inverse emulsion polymerization method. Scanning electron microscopy images confirmed the spherical morphology of the microgel particles as well as the homogeneous monodisperse particle size distribution.

DLS studies were carried out to determine and confirm the upper critical temperature behavior of the microgel dispersions. A dependence of the collapse temperature with respect to both the cross-linker and acrylic acid concentration was demonstrated. An increase of 10 and 8 °C, respectively, has been observed in the collapse temperature with respect to the polyacrylamide.

Concerning the rheological characterization, frequency sweep experiments described a more elastic than viscous system, suggesting that the system behaves as a colloidal gel. This conclusion was also confirmed by the up and down strain sweep measurements, in which the sample was deformed almost up to the crossover point and recover its elastic modulus. By assuming a certain structure, a systematic scaling theory for both the elastic modulus plateau and the limit of linearity of the microgel dispersions was applied. This theory confirmed that the solid-like behavior of the system was given by the formation of aggregates due to interactions among microgel particles. The fractal dimension of these aggregates is $D = 2.28$, indicating high density of microgel particles in the flocs.

Acknowledgment. Financial support from CICYT (MAT-2008-1073) and Fundación Domingo Martinez is acknowledged.

References and Notes

(1) Saunders, B. R.; Vincent, B. *Adv. Colloid Interface Sci.* **1999**, *80*, 1–25.
(2) Murray, M. J.; Snowden, M. J. *Adv. Colloid Interface Sci.* **1995**, *54*, 73–91.
(3) Wang, Q.; Zhao, Y.; Yang, Y.; Xu, H. *Colloid Polym. Sci.* **2007**, *285*, 515–521.
(4) Schmaljohann, D. *Adv. Drug Delivery Rev.* **2006**, *58*, 1655–1670.
(5) Hoare, T.; Pelton, R. *Macromolecules* **2007**, *40*, 670–678.
(6) Rubio Retama, J.; López-Ruiz, B.; López- Cabarcos, E. *Biomaterials* **2003**, *24*, 2965–2973.
(7) Garcia, A.; Marquez, M.; Cai, T.; Rosario, R.; Hu, Z.; Gust, D.; Hayes, M.; Vail, S.; Park, C. *Langmuir* **2007**, *23*, 224–229.
(8) Gan, D.; Lyon, L. A. *Macromolecules* **2002**, *35*, 9634–9639.
(9) Sáez-Martínez, V.; Pérez-Álvarez, L.; Herrero, M. T.; Hernández, E.; Katime, I. *Eur. Polym. J.* **2008**, *44*, 1309–1322.
(10) Pelton, R. *Adv. Colloid Interface Sci.* **2000**, *85*, 1–33.
(11) Imaz, A.; Forcada, J. *J. Polym. Sci., Part A: Polym. Chem.* **2008**, *46*, 2766–2775.
(12) Duracher, D.; Elaïssari, A.; Pichot, C. *Colloid Polym. Sci.* **1999**, *277*, 905–913.
(13) Saunders, B. R. *Langmuir* **2004**, *20*, 3925–3932.
(14) Xiao, X. C.; Chu, L. Y.; Chan, W. M.; Zhu, J. H. *Polymer* **2005**, *46*, 3199–3209.
(15) Bouillot, P.; Vincent, B. *Colloid Polym. Sci.* **2000**, *278*, 74–79.
(16) Owens, D. E.; Jian, Y.; Fang, J. E.; Slaughter, B. V.; Chen, Y. H.; Peppas, N. A. *Macromolecules* **2007**, *40*, 7306–7310.
(17) Wu, C.; Zhou, S. *Macromolecules* **1997**, *30*, 574–576.
(18) Xiao, X. C.; Chu, L. Y.; Chen, W. M.; Wang, S.; Li, Y. *Adv. Funct. Mater.* **2003**, *13*, 847–852.
(19) Stieger, M.; Richtering, W. *Macromolecules* **2003**, *36*, 8811–8818.
(20) Tan, B. H.; Tam, K. C.; Lam, Y. C.; Tan, C. B. *Adv. Colloid Interface Sci.* **2005**, *113*, 111–120.
(21) Senff, H.; Richtering, W. *J. Chem. Phys.* **1999**, *111*, 1705–1711.
(22) Senff, H.; Richtering, W. *Colloid Polym. Sci.* **2000**, *278*, 830–840.
(23) Brown, W. D.; Ball, R. C. *J. Phys. A* **1985**, *18*, 517–521.
(24) Shih, W.-H.; Shih, W. Y.; Kim, S.; Liu, J.; Aksay, I. *Phys. Rev. A* **1990**, *42*, 4772–4779.
(25) Fernández, E.; López, D.; López Cabarcos, E.; Mijangos, C. *Polymer* **2005**, *46*, 2211–2217.
(26) Hernández, R.; Sarafian, A.; López, D.; Mijangos, C. *Polymer* **2004**, *45*, 5543–5549.
(27) Hernández, R.; Mijangos, C.; López, D. *J. Polym. Sci., Polym. Phys.* **2005**, *43*, 1944–1949.
(28) Fernández, E.; López, D.; Mijangos, C.; Duskova-Smrckova, M.; Ilavsky, M.; Dusek, K. *J. Polym. Sci., Polym. Phys.* **2008**, *46*, 322–328.
(29) López, D.; Dahmani, M.; Mijangos, C.; Brulet, A.; Guenet, J. M. *Macromolecules* **1994**, *27*, 7415–7422.
(30) López, D.; Mijangos, C.; Muñoz, M. E.; Santamaria, A. *Macromolecules* **1996**, *29*, 7108–7115.
(31) Wu, H.; Morbidelli, M. *Langmuir* **2001**, *17*, 1030–1036.